

Revealing trends in catalytic activity of adatoms for hydrogen adsorption on carbon: a case study of graphene and carbon nanotube

Thomas Leiner^{1,*} and David Holec¹

¹*Department of Materials Science, Montanuniversität Leoben, Leoben, Austria*

(Dated: December 17, 2024)

The increasing demand for sustainable energy solutions necessitates advancements in hydrogen storage technologies. This study investigates the hydrogen adsorption characteristics of graphene and a (8,0) carbon nanotube (CNT) decorated with adatoms of various elements. Using molecular dynamics (MD) simulations and the universal interatomic potential 'PreFerred Potential' (PFP) implemented in the Matlantis framework, we explore the hydrogen storage capabilities of these doped carbon structures at 77 K. We analyze the adsorption efficiency based on the position of adatoms (top, bridge, and hollow sites) and find that the group II elements, such as calcium and strontium, exhibit significant hydrogen uptake. Additionally, light elements like lithium and sodium demonstrate enhanced gravimetric hydrogen storage due to their low atomic mass. Our findings provide insights into the potential of doped graphene and CNTs for efficient hydrogen storage applications.

I. INTRODUCTION

Due to the ecological problems related to the use of fossil fuels, alternative sources of energy and its storage have to be developed. One promising branch of ongoing research focuses on hydrogen. The most obvious advantage of hydrogen use instead of carbon-based (fossil) fuels is that after harvesting energy through reacting with oxygen, the “waste product” is climate-neutral water instead of carbon dioxide. Nonetheless, hydrogen technology still has to deal with a number of problems, ranging from economically and ecologically sensible hydrogen production over hydrogen storage in a reasonably small volume and with a high enough ratio of stored hydrogen per storage system mass, as well as developed transport infrastructure to get the hydrogen from the place of its production to the end user.

This work focuses on revealing trends related to the enhancement of graphene and carbon nanotubes' hydrogen storage capabilities by doping. Our particular interest is to scan over as many elements of the periodic system as possible. While it generally would be possible to simulate these systems with density functional theory (DFT) based approaches, as has been done in previous works [1–3], systematically iterating through the entire periodic table for dopants placed in various sites has not been done yet as it would require significant computational resources. On the other hand, molecular statics or dynamics would, in principle, also allow for the estimation of such energy-based trends, provided that interatomic potential exists. This was not the case until recently when a paradigm shift to data-driven materials science and machine learning opened the possibility of creating so-called universal potentials [4]. In the present work, we employ the PFP universal potential [5, 6]. Not only it allows to perform the desired simulations with

acceptable computational resources, but it also reveals systematic trends across the periodic table and enables to use of larger (than in DFT) simulation models and including finite temperature effects.

While there exist many hydrogen adsorption studies for doped graphene [1, 7–9] and 8-0 CNTs [3, 10–12], typically they focus on only one or a few dopants. Moreover, the conclusions are drawn using different system setups and methodologies, which makes comparing these studies difficult. This work aims to directly compare the effect of the doping elements across (almost) the entire periodic table with each other.

II. METHODS

A. Structural models

As the systems of interest, we chose two fundamental carbon structures, a graphene sheet and a carbon nanotube (CNT) rolled in the 8-0 configuration [13].

On a graphene sheet, it is possible to place an additional adatom in three different (high-symmetry) places: in the middle of the carbon hexagons (hollow site), above a carbon-carbon bond (bridge site), or on top of a carbon atom (top site), as visualized in Fig. 1a–c. The simulation model of the graphene sheet was contained in an $86 \times 75 \times 26 \text{ \AA}^3$ simulation cell, corresponding to a 35×35 supercell of graphene (2450 C atoms). In total, 49 doping atoms were placed in the desired positions (hole, bridge, top), followed by an introduction of 392 hydrogen molecules placed on a regular grid in a vacuum region away from the graphene sheet. The resulting model contained 3283 atoms.

Analogous sites were also chosen for the placement of the adatoms in the CNT case (Fig. 2), with the exception that there are two unequal carbon-carbon bonds and therefore two different bridge sites: one which we designate as diagonal (Fig. 2b) and the other horizontal

* thomas.leiner@unileoben.ac.at

(Fig. 2c).

The 8-0 CNT with a radius of $R = 3.15 \text{ \AA}$ and a C-C bond length of 1.421 \AA was created using an online tool [14]. Four identical axes-aligned CNTs, each composed of 196 atoms, were placed in a $40 \times 40 \times 26.6 \text{ \AA}^3$ simulation box. Subsequently, 16 adatoms were introduced (4 on each CNT), resulting in a similar atomic concentration (2 at.%) as in the graphene case. Finally, the empty space was filled with 128 H_2 molecules randomly placed, thereby yielding models with 1040 atoms.

In all cases, the adatoms were evenly spaced to minimize the influence a dopant-dopant interaction could have. An example of a simulation cell is given in Fig. 3. Periodic boundary conditions were applied in all three spatial directions.

B. Simulation environment

For our work, we chose a universal potential called ‘Preferred Potential’ (PFP) provided by the Preferred Computational Chemistry (PFCC). It describes interactions between 72 different elements of the periodic table and is made accessible with a cloud simulation platform called MatlantisTM [5, 6].

PFP is a neural network potential (NNP) based on the TeaNet architecture [15] with an additional Morse-style two-body potential term for short-range repulsion. Its training and validation dataset was gener-

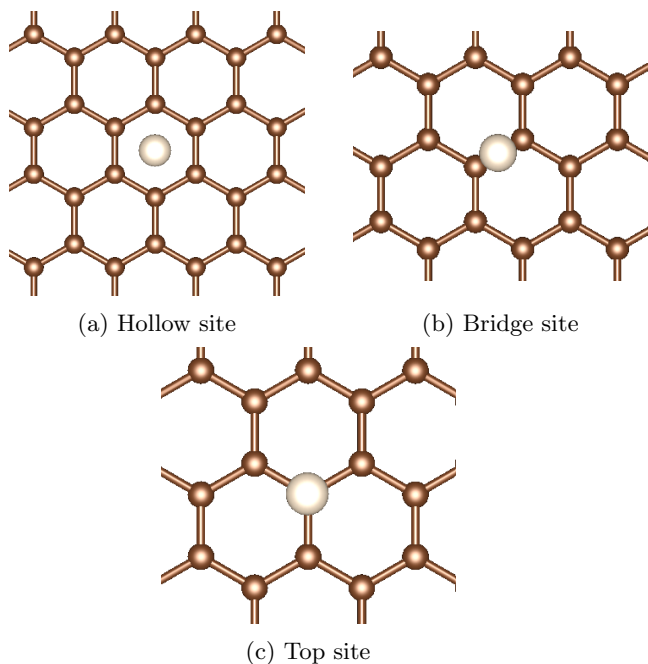


FIG. 1: Structures with graphene basis: (a) hollow site, (b) bridge site, (c) top site. The adatom is represented by the white atom.

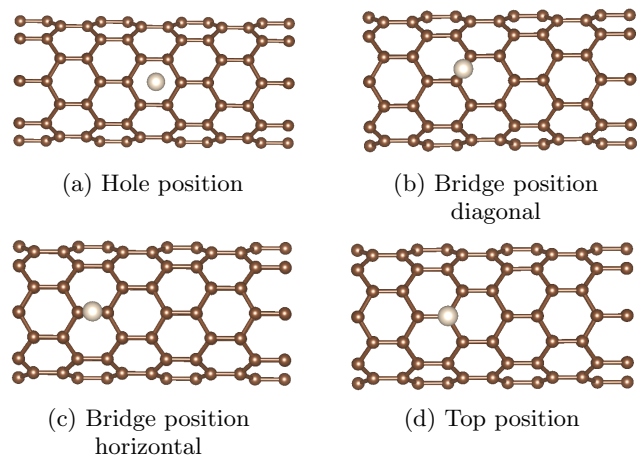


FIG. 2: Structures with CNT basis: (a) hole position, (b) bridge position diagonal, (c) bridge position horizontal, (d) top position. The dopant is represented by the white atom.

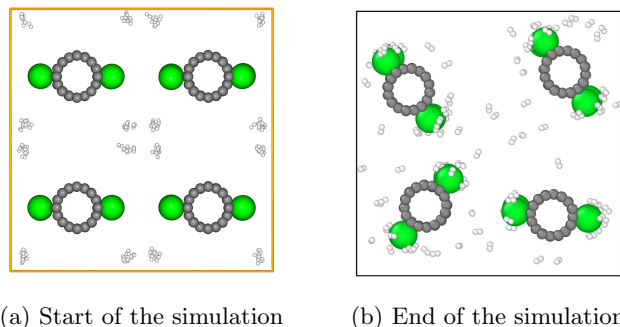


FIG. 3: Simulation cell with four 8-0 CNTs (grey) with adsorbed Strontium atoms (green) in the hole position. Adsorbed and free hydrogen molecules in white.

ated using the Vienna Ab-initio Simulation Package (VASP) [16, 17] with a Perdew–Burke–Ernzerhof (PBE) generalized-gradient approximation for the exchange–correlation functional [18]. The projector-augmented wave (PAW) [19, 20] method and plane-wave basis set were used together with the kinetic energy cutoff set to 520 eV. Gaussian smearing was applied with a smearing width of 0.05 eV. The k -point density was set to 1000 k -points per reciprocal atom [5]. The energy of the system, atomic forces, and atomic charges are used for the training procedure. For additional information about the generation of the potential, see the original papers [5, 6]. During all PFP calculations, a van-der-Waals D3 correction by Grimme et al. [21] was applied.

Motivated by experimental practice [22], the temperature of our molecular dynamics simulations was set to 77 K. The MD simulations were performed using an NVT

ensemble, using a Berendsen thermostat integrator [23]. They ran for 50,000 timesteps, each 1 fs long, yielding a total simulation time of 50 ps.

All evaluations were done using the integrated Jupyter/python-based Matlantis environment, including also the ASE tools [24]. A hydrogen atom was considered adsorbed to an adatom if their mutual distance was shorter than 3 \AA .

III. RESULTS AND DISCUSSION

In order to have representative results, we made sure that the simulations reached an equilibrated state after the 50,000 timesteps, as measured by a constant amount of hydrogen molecules adsorbed to the dopant elements (i.e., on average, an equal amount of hydrogen adsorbs and desorbs from the adatom sites).

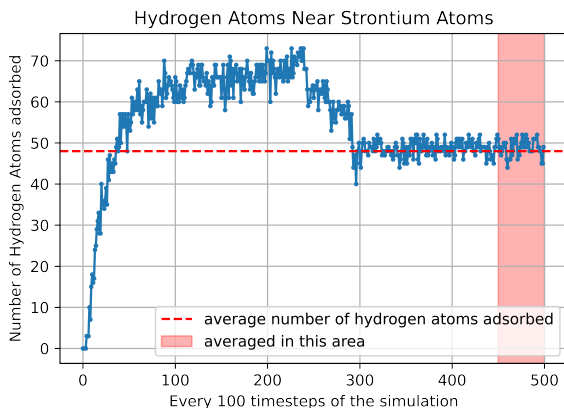


FIG. 4: Number of hydrogen atoms adsorbed to Strontium over the entirety of the simulation, with a datapoint every hundred timesteps.

To quantify the number the number of adsorbed hydrogen molecules, we summed up the number of hydrogen atoms within 3 \AA of the dopant. The representative number used to extract trends over the period table is then obtained as the time average over the last 5,000 timesteps (5 ps) of the simulation. An example that shows that the amount of adsorbed hydrogen atoms is in thermodynamic equilibrium is seen in Fig. 4, with the average number of adsorbed hydrogen atoms on Strontium adatoms being ≈ 48 (red dashed line) with fluctuations of $\approx 5\%$ at the end of the simulation (red shaded area).

The case-resolved average adsorption capacities of individual adatoms are given in Supplementary Material. Since the different sites for graphene and for the CNT show qualitatively the same trends, we averaged them and presented them in the form of heatmaps in Figs. 5 and 6. The best performing adatoms, i.e. those binding the highest number of H atoms, are alkali earth metals (calcium, strontium), some early transition metals (scandium, titanium, hafnium, (yttrium), (niobium))

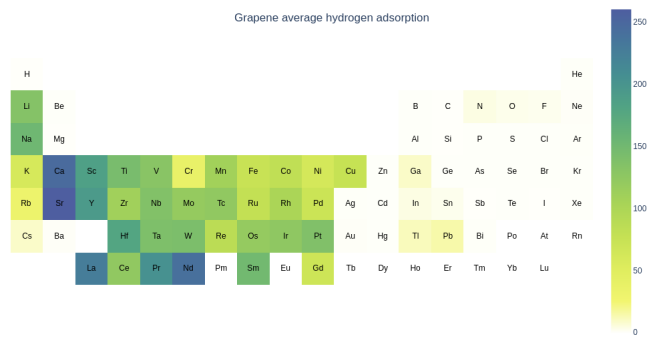


FIG. 5: Adsorption heatmap on graphene sheet with active adatoms.

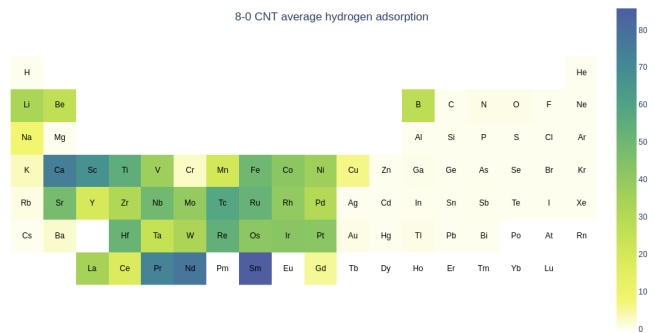


FIG. 6: Adsorption heatmap on a 8-0 CNT with active adatoms.

and some lanthanides (praseodymium, neodymium, (lanthanum), (samarium)). Although promising, technetium is rather impractical due to its radioactivity.

Figures 7 and 8 show the average gravimetric uptake of hydrogen for the graphene and CNT cases. This is an important parameter in hydrogen storage applications, as the system size and weight are critical for practical hydrogen storage applications. To calculate it, the number of absorbed H atoms was divided by the atomic mass of the adatom elements. This shifts the spotlight towards light elements, as seen by the peaks for lithium, sodium and calcium, which thereby outperform the strongly attractive but heavy adatoms such as lanthanum, neodymium or samarium. Significant differences between graphene and the CNT are the higher peak for sodium in Fig. 7 and the high values for boron and beryllium in Fig. 8. Last but not least, strontium seems to be significantly enhancing the H adsorption only in the case of graphene (Fig. 7). As a general trend for both graphene and CNT cases, a declining trend in gravimetric capacity is predicted within each individual period (individual periods marked with dashed red lines). Note also the different y -axis scales in both figures, suggesting the flat graphene is 3–4 times more efficient than the CNT.

Two effects are reported in the literature concerning the hydrogen uptake of doped carbon structures,

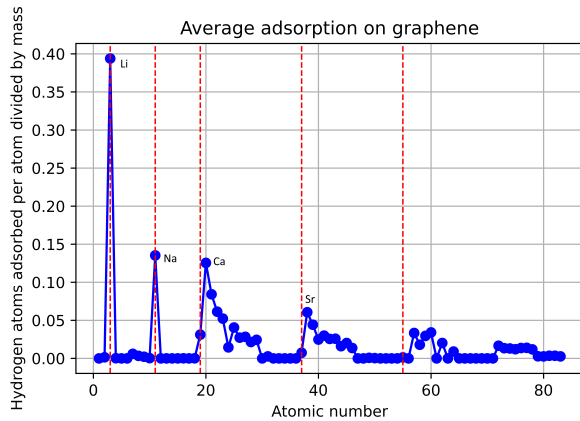


FIG. 7: Gravimetric uptake of hydrogen on graphene with active adatoms.

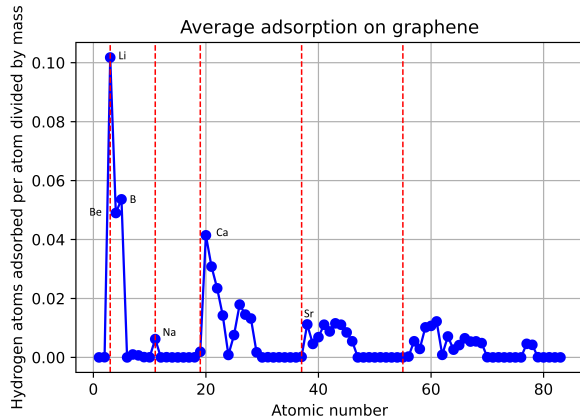


FIG. 8: Gravimetric uptake of hydrogen on 8-0 CNT with active adatoms.

namely hydrogen spillover [25] and the Kubas-type interaction [26]. The hydrogen spillover is mainly reported for defective carbon structures. In agreement with this observation, we did not observe it during our simulations

employing pristine carbon structures. Another reason for not observing the hydrogen spillover might be the limited simulation time, which, together with the limited kinetics at a low temperature of 77 K, do not allow for spillover to occur. This study could be expanded for future research by incorporating defective graphene planes, such as those with Stone–Wales defects or sheet edges, to investigate hydrogen spillover more closely. A study of the electronic structure of a local environment representing an adatom with an adsorbed hydrogen could reveal the role of the Kubas-type interaction in the adsorption enhancement. For this, an electronic-structure code would be necessary, which goes beyond the capabilities of the used universal potential. Clustering was reported for transition metal dopants [27, 28], which poses an additional technical problem synthesizing the material, when considering the gravimetric and total hydrogen uptake capability of the materials. Therefore, this topic would also be interesting to include in the follow-up studies.

IV. CONCLUSIONS

Hydrogen technologies are considered to be part of the solution to the problems related to climate change. In this paper, we present a systematic theoretical investigation of the catalytic activity of adatoms enhanced hydrogen uptake by carbon-based nanostructures, namely graphene and 8-0 CNT. To do so, we performed a molecular dynamics study employing a recently published neural network interatomic potential fitted to DFT-GGA data. Our calculations identified multiple atomic species, such as lithium, boron, beryllium, calcium, and strontium, that can lead to improved gravimetric hydrogen uptake.

ACKNOWLEDGEMENTS

This work is a part of the Strategic Core Research Area (SCoRe A+ Hydrogen and Carbon) and is receiving financial support from Montanuniversität Leoben, Austria.

-
- [1] D. Holec, N. Kostoglou, C. Tampaxis, B. Babic, C. Mitterer, and C. Rebholz, Theory-guided metal-decoration of nanoporous carbon for hydrogen storage applications, *Surf. Coat. Technol.* **351**, 42 (2018).
 - [2] H.-Y. Zhuo, X. Zhang, J.-X. Liang, Q. Yu, H. Xiao, and J. Li, Theoretical understandings of graphene-based metal single-atom catalysts: stability and catalytic performance, *Chemical reviews* **120**, 12315 (2020).
 - [3] J. Lyu, V. Kudiiarov, and A. Lider, An overview of the recent progress in modifications of carbon nanotubes for hydrogen adsorption, *Nanomaterials* **10**, 255 (2020).
 - [4] J. Riebesell, R. E. A. Goodall, P. Benner, Y. Chiang, B. Deng, A. A. Lee, A. Jain, and K. A. Persson, Mat-

bench discovery – a framework to evaluate machine learning crystal stability predictions, *arXiv [cond-mat.mtrl-sci]* (2023), [arXiv:2308.14920 \[cond-mat.mtrl-sci\]](https://arxiv.org/abs/2308.14920).

- [5] S. Takamoto, C. Shinagawa, D. Motoki, K. Nakago, W. Li, I. Kurata, T. Watanabe, Y. Yayama, H. Iriguchi, Y. Asano, *et al.*, Towards universal neural network potential for material discovery applicable to arbitrary combination of 45 elements, *Nature Communications* **13**, 2991 (2022).
- [6] S. Takamoto, D. Okano, Q.-J. Li, and J. Li, Towards universal neural network interatomic potential, *Journal of Materiomics* **9**, 447 (2023).

- [7] R. Miwa, T. B. Martins, and A. Fazio, Hydrogen adsorption on boron doped graphene: an ab initio study, *Nanotechnology* **19**, 155708 (2008).
- [8] C. Tabtimsai, W. Rakrai, and B. Wannoo, Hydrogen adsorption on graphene sheets doped with group 8b transition metal: a dft investigation, *Vacuum* **139**, 101 (2017).
- [9] V. Jain and B. Kandasubramanian, Functionalized graphene materials for hydrogen storage, *Journal of Materials Science* **55**, 1865 (2020).
- [10] H. Nakano, H. Ohta, A. Yokoe, K. Doi, and A. Tachibana, First-principle molecular-dynamics study of hydrogen adsorption on an aluminum-doped carbon nanotube, *Journal of Power Sources* **163**, 125 (2006), special issue including selected papers presented at the Second International Conference on Polymer Batteries and Fuel Cells together with regular papers.
- [11] B. J. Nagare, D. Habale, S. Chacko, and S. Ghosh, Hydrogen adsorption on na-swcnt systems, *Journal of Materials Chemistry* **22**, 22013 (2012).
- [12] V. Verdinelli, E. German, C. R. Luna, J. M. Marchetti, M. A. Volpe, and A. Juan, Theoretical study of hydrogen adsorption on ru-decorated (8, 0) single-walled carbon nanotube, *The Journal of Physical Chemistry C* **118**, 27672 (2014).
- [13] S. Iijima, Helical microtubules of graphitic carbon, *nature* **354**, 56 (1991).
- [14] J. T. Frey and D. J. Doren, Tubegen 3.4 (web-interface), <http://turin.nss.udel.edu/research/tubegenonline.html> (2011), university of Delaware, Newark DE.
- [15] S. Takamoto, S. Izumi, and J. Li, Teanet: Universal neural network interatomic potential inspired by iterative electronic relaxations, *Computational Materials Science* **207**, 111280 (2022).
- [16] G. Kresse and J. Furthmüller, Efficiency of ab-initio total energy calculations for metals and semiconductors using a plane-wave basis set, *Computational materials science* **6**, 15 (1996).
- [17] G. Kresse and J. Furthmüller, Efficient iterative schemes for ab initio total-energy calculations using a plane-wave basis set, *Physical review B* **54**, 11169 (1996).
- [18] J. P. Perdew, K. Burke, and M. Ernzerhof, Generalized gradient approximation made simple, *Physical review letters* **77**, 3865 (1996).
- [19] P. E. Blöchl, Projector augmented-wave method, *Physical review B* **50**, 17953 (1994).
- [20] G. Kresse and D. Joubert, From ultrasoft pseudopotentials to the projector augmented-wave method, *Physical review b* **59**, 1758 (1999).
- [21] S. Grimme, J. Antony, S. Ehrlich, and H. Krieg, A consistent and accurate ab initio parametrization of density functional dispersion correction (dft-d) for the 94 elements h-pu, *J. Chem. Phys.* **132**, 154104 (2010).
- [22] N. Kostoglou, C.-W. Liao, C.-Y. Wang, J. N. Kondo, C. Tampaxis, T. Steriotis, K. Giannakopoulos, A. G. Kontos, S. Hinder, M. Baker, E. Bousser, A. Matthews, C. Rebholz, and C. Mitterer, Effect of pt nanoparticle decoration on the h2 storage performance of plasma-derived nanoporous graphene, *Carbon* **171**, 294 (2021).
- [23] H. J. Berendsen, J. v. Postma, W. F. Van Gunsteren, A. DiNola, and J. R. Haak, Molecular dynamics with coupling to an external bath, *The Journal of chemical physics* **81**, 3684 (1984).
- [24] A. H. Larsen, J. J. Mortensen, J. Blomqvist, I. E. Castelli, R. Christensen, M. Dułak, J. Friis, M. N. Groves, B. Hammer, C. Hargus, E. D. Hermes, P. C. Jennings, P. B. Jensen, J. Kermode, J. R. Kitchin, E. L. Kolsbjerg, J. Kubal, K. Kaasbjerg, S. Lysgaard, J. B. Maronsson, T. Maxson, T. Olsen, L. Pastewka, A. Peterson, C. Rostgaard, J. Schiøtz, O. Schütt, M. Strange, K. S. Thygesen, T. Vegge, L. Vilhelmsen, M. Walter, Z. Zeng, and K. W. Jacobsen, The atomic simulation environment—a python library for working with atoms, *J. Phys. Condens. Matter* **29**, 273002 (2017).
- [25] D. S. Pyle, E. M. Gray, and C. Webb, Hydrogen storage in carbon nanostructures via spillover, *International Journal of Hydrogen Energy* **41**, 19098 (2016).
- [26] G. J. Kubas, Molecular hydrogen complexes: coordination of a sigma. bond to transition metals, *Accounts of Chemical Research* **21**, 120 (1988).
- [27] S. Lambie, K. G. Steenbergen, N. Gaston, and B. Paulus, Clustering of metal dopants in defect sites of graphene-based materials, *Physical Chemistry Chemical Physics* **24**, 98 (2022).
- [28] Q. Sun, Q. Wang, P. Jena, and Y. Kawazoe, Clustering of ti on a c60 surface and its effect on hydrogen storage, *Journal of the American Chemical Society* **127**, 14582 (2005).

Supplementary Information
Revealing trends in catalytic activity of adatoms for
hydrogen adsorption on carbon: a case study of
graphene and carbon nanotube

Thomas Leiner and David Holec
Department of Materials Science, Montanuniversität Leoben, Leoben, Austria

December 17, 2024

arXiv:2412.11960v1 [cond-mat.mtrl-sci] 16 Dec 2024

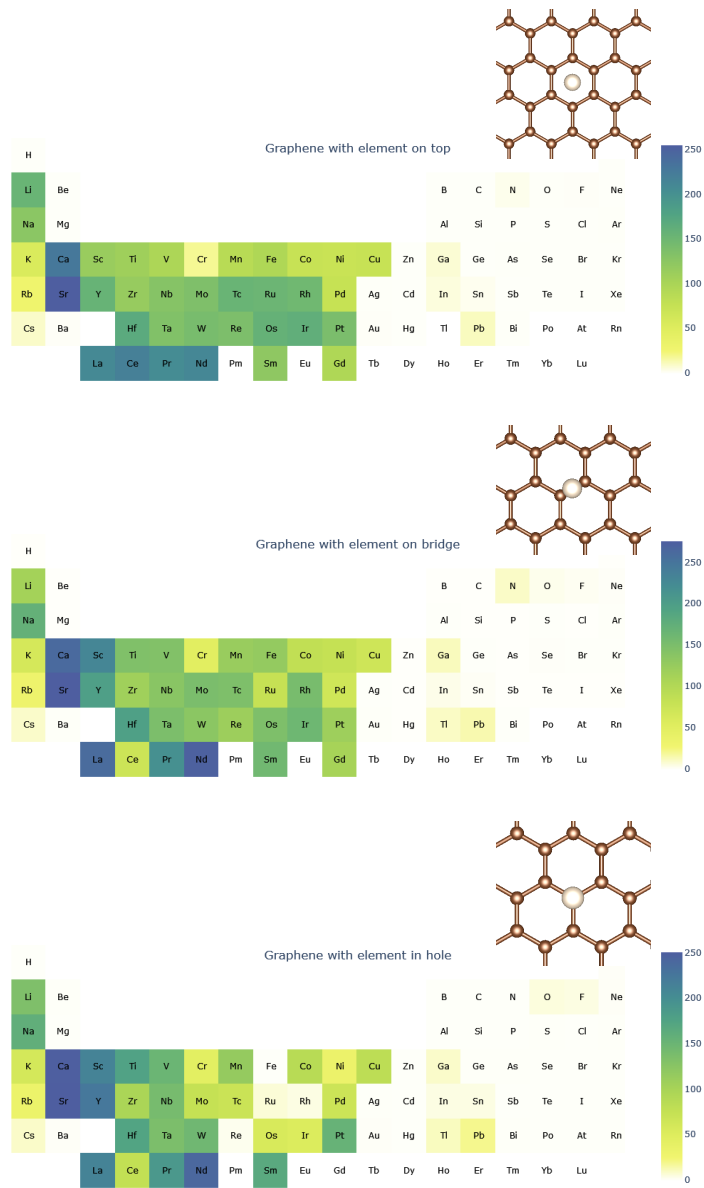


Figure 1: Adsorption heatmaps on graphene. The images show different configurations of graphene: in a hole, on a bridge, and on top.

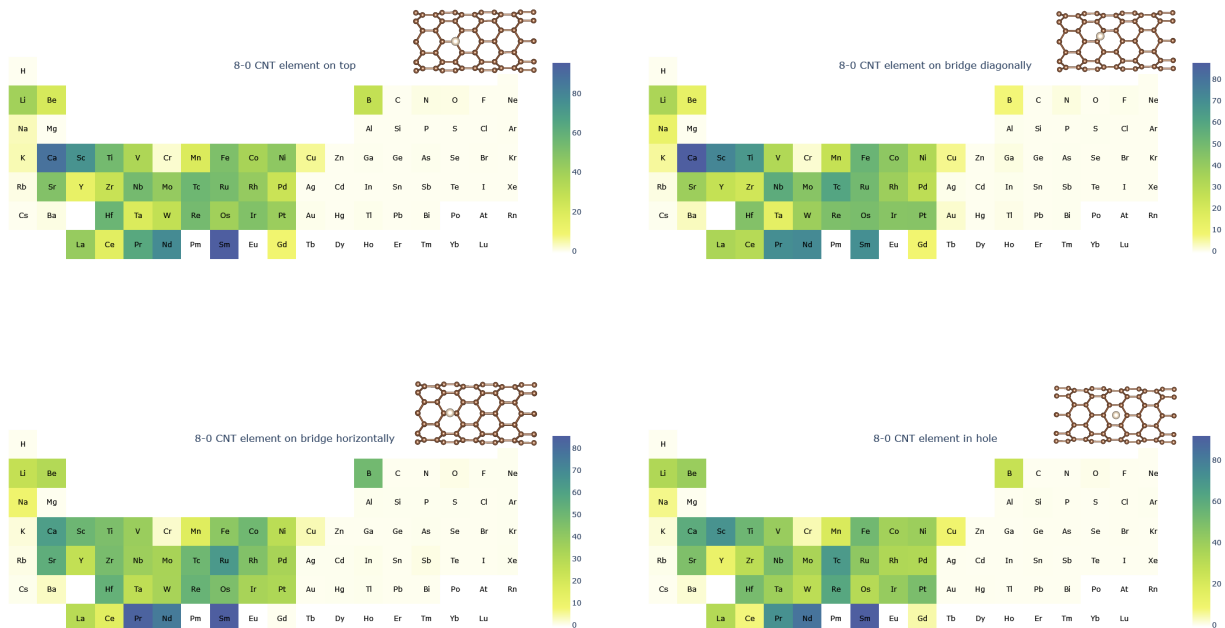


Figure 2: Adsorption heatmaps on CNT. The images show different configurations of graphene: in a hole, on a bridge diagonally and horizontally, and on top.